# $Al_2O_3$-TiC/1Cr18Ni9Ti 扩散焊接头应力分布

沈孝芹[1,2]， 李亚江[1,3]， Puchkov U A[3]， 王 娟[1]， 黄万群[1]

（1. 山东大学 材料液态结构及其遗传性教育部重点实验室，济南 250061；
2. 山东建筑大学 机电学院，济南 250101；
3. 莫斯科鲍曼国立科技大学，俄罗斯 莫斯科 105005）

摘 要：用有限元方法计算了 $Al_2O_3$-TiC/1Cr18Ni9Ti 扩散焊接头的应力分布，研究了加热温度、压力和中间层对应力分布的影响。结果表明，残余轴向应力和剪切应力在试样边缘处梯度都较大，靠近中心轴，应力分布比较均匀，最大剪切应力出现在 $Al_2O_3$-TiC/中间层界面处。在扩散焊冷却过程中，$Al_2O_3$-TiC/1Cr18Ni9Ti 扩散焊接头最大轴向拉应力先是出现在边缘陶瓷侧，随着温度的降低，逐渐向试样中心靠近，应力值也逐渐增大。加热温度越低，轴向压应力越大。压力越大，最大轴向拉应力越小，压应力越大，但压力对剪切应力的影响较小。使用 Ti-Cu-Ti 复合中间层比使用 Ti 中间层可降低最大轴向压应力和最大剪切应力。

关键词：$Al_2O_3$-TiC；不锈钢；扩散焊；应力

中图分类号：TG44 文献标识码：A 文章编号：0253－360X(2008)10－0041－04

沈孝芹

## 0 序 言

$Al_2O_3$-TiC 复合陶瓷是由 $Al_2O_3$ 基体及分布在其中的 TiC 颗粒组成的复合陶瓷，可广泛用作高温发热体、火花塞和耐磨材料，尤其是用它制成的切削刀具的可切削速度比硬质合金刀具高得多，已用作铸铁和高硬度钢的高速切铣加工[1]。但陶瓷材料固有的硬性和脆性使其难以加工、难以制成大型或形状复杂的构件，将 $Al_2O_3$-TiC 复合陶瓷与钢用扩散焊方法连接起来制成复合构件，对于改善受力状态、结构内部应力分布、提高韧性和拓宽 $Al_2O_3$-TiC 复合陶瓷的使用范围具有重要的意义。

陶瓷和金属的线膨胀系数和弹性模量差别很大，在焊接加热和冷却的过程中，接头界面附近产生较大的热应力和残余应力。为缓解陶瓷与金属接头残余应力，常采用中间层[2,3]。由于扩散焊接头中应力分布比较复杂，梯度较大，难以实现准确测量，而且试验工作量较大，因此常采用解析法和有限元方法进行分析计算[4－6]。用 ANSYS 有限元软件计算了不同加热温度、不同压力和不同中间层时扩散连接 $Al_2O_3$-TiC 复合陶瓷/1Cr18Ni9Ti 不锈钢的接头应力分布，计算结果可对 $Al_2O_3$-TiC 复合陶瓷/不锈钢扩散连接制定合理的工艺参数提供理论指导。

收稿日期：2007－11－23
基金项目：山东省优秀中青年基金资助项目(2006BS04004)

## 1 试验条件与计算方法

试验材料为 $Al_2O_3$-TiC 复合陶瓷和 1Cr18Ni9Ti 不锈钢。其中 $Al_2O_3$-TiC 复合陶瓷是通过热压烧结工艺（HPS）制成的 $\phi$50 mm × 3 mm 的圆片试样，1Cr18Ni9Ti 不锈钢的待连接试样尺寸为 $\phi$50 mm × 1 mm。将 0.1 mm 的 Ti-Cu-Ti 复合中间层（其中 Ti 0.02 mm，Cu 0.06 mm）置于 $Al_2O_3$-TiC 复合陶瓷和 1Cr18Ni9Ti 不锈钢之间，放于真空室中进行扩散连接。加热温度为 1 100～1 160 ℃，保温时间为 45～60 min，连接压力为 5～30 MPa，真空度 $p_0=10^{-5}$ Pa。扩散焊接头示意图如图 1a 所示。

在进行 $Al_2O_3$-TiC/1Cr18Ni9Ti 扩散焊接头应力分析时，$Al_2O_3$-TiC 陶瓷看作是弹性体，不锈钢和中间层为理想弹塑性体，材料遵循 Von Mises 屈服准则和等向强化假定。有限元计算中材料热物理性能参数见表 1[7,8]。根据工件的尺寸建立有限元模型，由于连接试样为轴对称，因此选取任一子午面进行分析，选用四节点轴对称单元划分网格。为使计算结果更精确，在扩散焊界面附近区域对计算模型进行网格加密划分，扩散焊接头处的有限元网格划分如图 1b 所示，图中 $z$ 为试样中心轴，$r$ 为距 $z$ 轴距离。

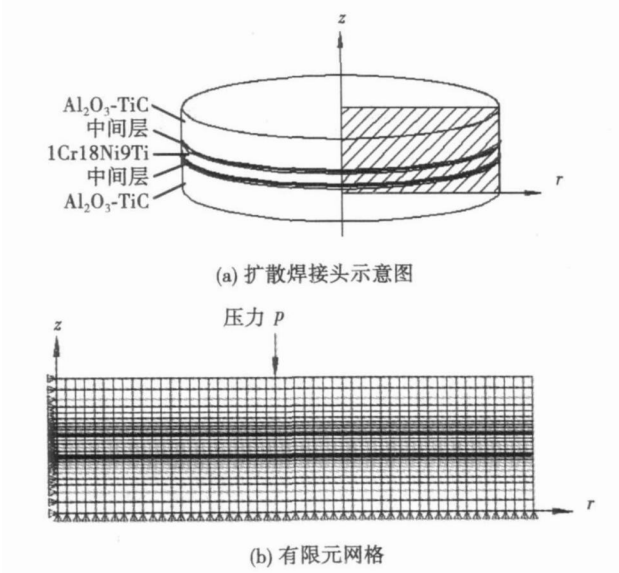


图 1 扩散焊接头示意图及有限元网格

Fig. 1 Schematic of diffusion bonded joint and the FEM mesh

表 1 有限元计算中所采用的材料参数

Table 1 Material properties employed in FEM

| 材料 | 温度 $T$/℃ | 弹性模量 $E$/GPa | 泊松比 $\mu$ | 线膨胀系数 $\alpha_l$/($10^{-6}$ ℃$^{-1}$) | 屈服强度 $R_{eL}$/MPa |
|---|---|---|---|---|---|
| $Al_2O_3$-TiC | 25 | 375 | 0.33 | 8.5 | — |
| 1Cr18Ni9Ti | 25 | 198 | 0.3 | — | 235 |
| 1Cr18Ni9Ti | 100 | 194 | 0.3 | 16.6 | — |
| 1Cr18Ni9Ti | 600 | 157 | 0.3 | 18.2 | 176 |
| 1Cr18Ni9Ti | 700 | 147 | 0.3 | 18.6 | 127 |
| Cu | 25 | 128.7 | 0.3 | 17.1 | 71 |
| Ti | 25 | 109.2 | 0.27 | 8.2 | 140 |

由于实际焊接过程中，下面的陶瓷片放置在压头支撑块上，所以有限元分析中采用的边界条件是陶瓷底面 $z=0$ 处施加 $z$ 向位移为零的约束，$z$ 轴为对称轴。外加载荷包括连接件的上端面施加的压力载荷 $p$ 和温度载荷。

将模型初始温度设置为扩散焊的加热温度，计算得出从加热温度降至室温时扩散焊接头处的应力分布。计算过程中，根据实际冷却过程，温度较高时，冷却速度较大；温度越低，冷却速度越小。

## 2 计算结果及分析

### 2.1 轴向应力和剪切应力的分布

图 2 是以 Ti-Cu-Ti 为中间层，压力 $p=15$ MPa，加热温度为 1 130 ℃时 $Al_2O_3$-TiC/1Cr18Ni9Ti 扩散焊接头残余轴向应力和剪切应力的分布。由图 2 可见，接头边缘处残余轴向应力和剪切应力梯度都较大，靠近对称轴应力分布比较均匀。最大轴向残余拉应力在距边缘约 5 mm 处，最大残余压应力在边缘不锈钢处。残余剪切应力最大值在上下陶瓷/中间层的界面边缘处，两侧大小相等，方向相反。因此当有外加剪切方向载荷施加在接头上时，断裂易从此处断开。

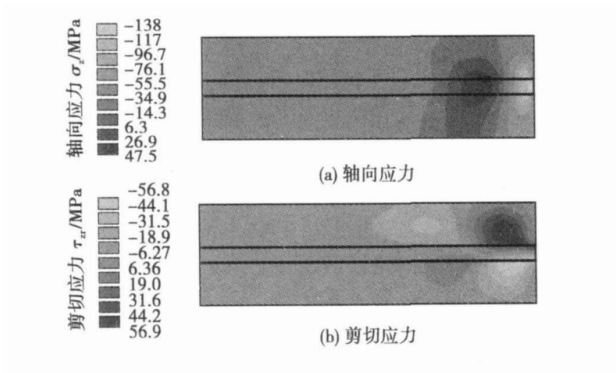


图 2 $Al_2O_3$-TiC/1Cr18Ni9Ti 扩散焊接头应力分布

Fig. 2 Stress distribution in $Al_2O_3$-TiC/1Cr18Ni9Ti diffusion bonded joint

图 3 是 $Al_2O_3$-TiC/1Cr18Ni9Ti 扩散焊接头(接头抗剪强度为 83 MPa)的剪切断口形貌。由图 3 可知：在 $Al_2O_3$-TiC/1Cr18Ni9Ti 接头的断裂表面存在两个明显的区域，用 X 射线衍射物相(XRD)分析可知，断面上的化合物是 $Al_2O_3$，TiC 和中间层反应产物 $Ti_3Al$，$Al_9Cr_4$ 等，表明在外剪切力作用时，裂纹容易从边缘剪切残余应力较大的界面处产生，并向近边缘处轴向残余拉伸应力较大的陶瓷侧扩展，这与上述计算结果相吻合。

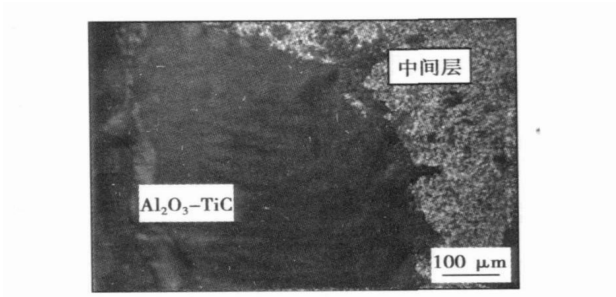


图 3 接头(1Cr18Ni9Ti 不锈钢一侧)断口形貌

Fig. 3 Fracture surface of joint (1Cr18Ni9Ti side)

图 4 是接头边缘附近轴向应力在冷却过程中的变化。由图 4 可见，在冷却过程中，最大轴向拉应力先是出现在接头边缘陶瓷侧，随着温度的降低，最大轴向拉应力逐渐远离边缘，应力值也逐渐增大。最大轴向压应力始终处于不锈钢的厚度中间靠近边缘

处，随着温度的降低，应力值也逐渐增大。

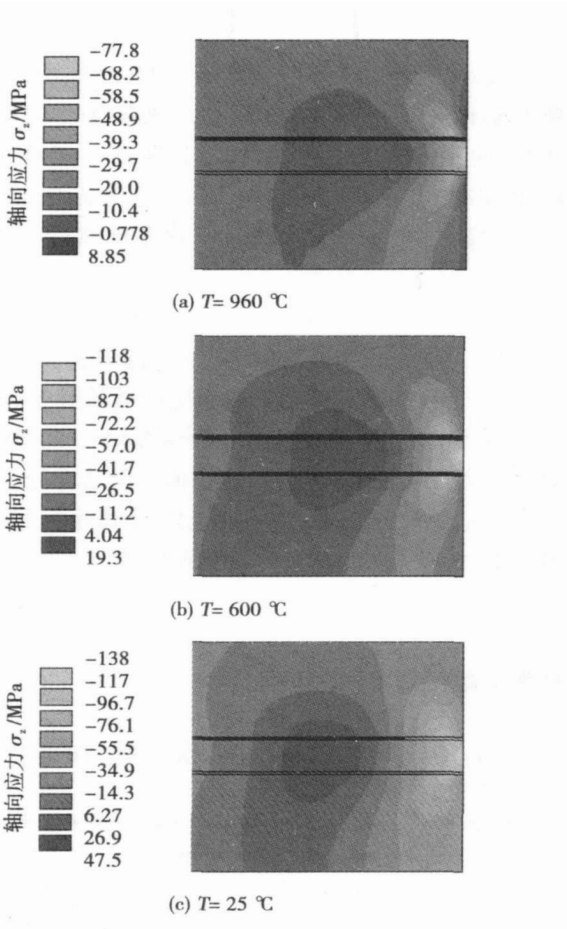


图 4　接头边缘处轴向应力在冷却过程中的变化

Fig. 4　Variation of axial stress in joint edge during cooling

## 2.2　加热温度对应力分布的影响

图5 是以 Ti-Cu-Ti 为中间层，压力 $p$＝15 MPa，加热温度分别为1 100，1 130，1 160和1 000 ℃时 $Al_2O_3$-TiC/Ti 界面处轴向应力和剪切应力的分布曲线。由图 5a 可知，轴向应力在试样边缘附近变化较大，最大轴向拉应力在距边缘4.5 mm处，约40 MPa；最大轴向压应力在距外边缘0.5 mm处，约120 MPa。在一定范围内，加热温度对残余应力的影响不大，加热温度为1 100，1 130和1 160 ℃时，残余轴向应力和剪切应力的值基本接近。为了对比，还计算了加热温度为1 000 ℃时残余应力的值，由图可见，加热温度越低，轴向压应力的值越大。由图 5b 可见，最大剪切应力发生在距边缘0.5 mm处，在近对称轴处，剪切应力值很小。

## 2.3　压力对应力分布的影响

图6 是采用 Ti-Cu-Ti 复合中间层、加热温度为1 130 ℃时在不同压力作用下应力分布情况。由图6a

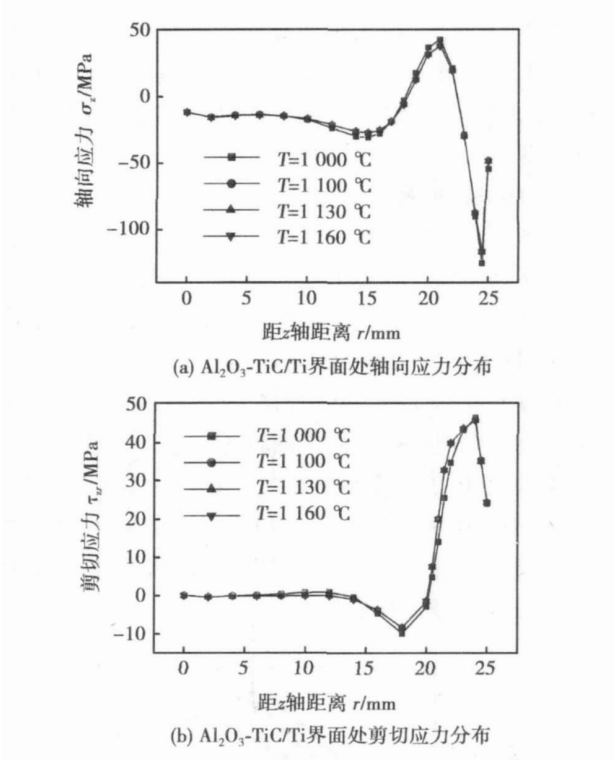


图 5　加热温度对试样接头应力分布的影响

Fig. 5　Influence of bonding temperature on stress in $Al_2O_3$-TiC/Ti interlayer

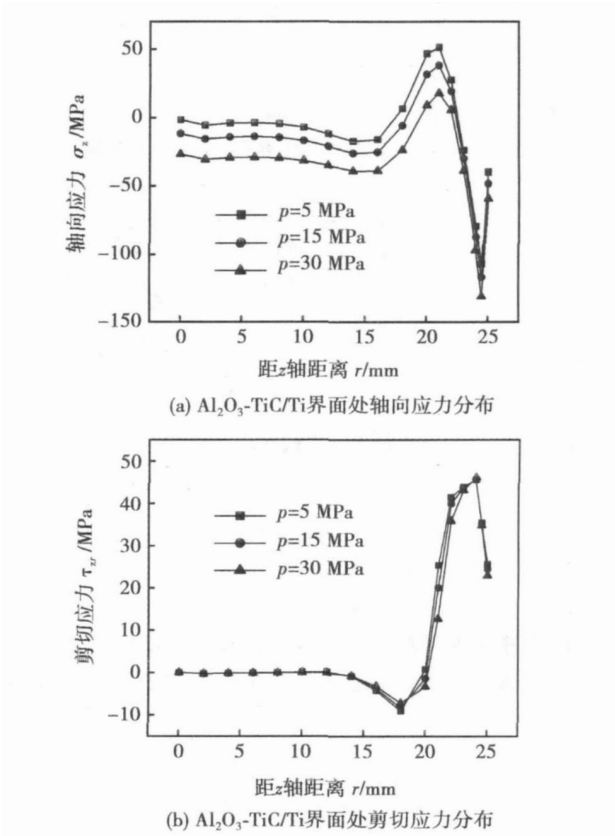


图 6　压力对 $Al_2O_3$-TiC/Ti 界面处应力分布的影响

Fig. 6　Influence of pressure on stress in $Al_2O_3$-TiC/Ti interlayer

可见,压力越大,最大轴向拉应力的值越小,压应力值越大。由图 6b 可见,压力对剪切应力的影响较小,压力增大,剪切应力最大值略有减小,最大值移向边缘处。

### 2.4 中间层的影响

图 7 是加热温度为 1 130 ℃,压力 $p=15$ MPa,采用不同中间层时应力分布情况。由图 7a 可见,使用 Ti(0.1 mm)中间层时,界面处最大轴向压应力最大,但最大轴向拉应力最小;使用 Ti-Cu-Ti(其中 Ti 层厚度为 0.02 mm,Cu 层厚度为 0.06 mm,总厚度为 0.1 mm)中间层可使最大轴向压应力减小且最大拉应力的位置更远离边缘处。由图 7b 可见,使用 Ti-Cu-Ti 中间层剪切应力的最大值比使用 Ti 中间层减小21 MPa。用 Cu (0.1 mm)作中间层轴向应力和剪切应力的值都有所减小。

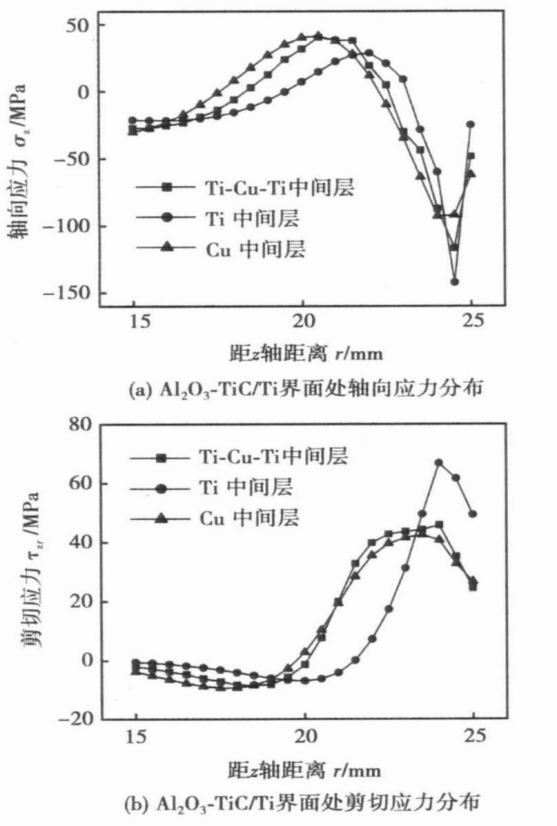


(a) $Al_2O_3$-TiC/Ti界面处轴向应力分布

(b) $Al_2O_3$-TiC/Ti界面处剪切应力分布

图 7 中间层对 $Al_2O_3$-TiC/中间层界面处应力分布的影响

Fig. 7 Influence of interlayer on stress in $Al_2O_3$-TiC/interlayer

## 3 结 论

(1) 在接头边缘附近残余轴向应力和剪切应力梯度都较大,剪切应力最大值出现在 $Al_2O_3$-TiC/中间层的界面处。在冷却过程中,$Al_2O_3$-TiC/1Cr18Ni9Ti 扩散焊接头最大轴向拉应力先是出现在边缘陶瓷侧,随着温度的降低,逐渐向试样中心移动,应力值也逐渐增大。

(2) 在一定范围内,加热温度对残余应力的影响不大,加热温度越低,轴向压应力的值越大。

(3) 压力越大,最大轴向拉应力的值越小,压应力值越大。压力对剪切应力的影响较小,压力增大,剪切应力最大值略有减小,最大值移向边缘处。

(4) 使用 Ti-Cu-Ti 中间层比使用 Ti 中间层可使最大轴向压应力减小,最大剪切应力的值减小 21 MPa。

参考文献:

[1] 蔡克峰,南策文,袁润章. $Al_2O_3$-TiC 复合陶瓷的研究进展[J]. 材料导报,1995,9(1):45—48.

[2] Dilemando T, Maurizio F, Gert Den O. Diffusion bonding of aluminium oxide to stainless steel using stress relief interlayers[J]. Materials Science and Engineering, 2002, 337(1—2): 287—296.

[3] 冯吉才,刘玉莉,张九海,等. 碳化硅陶瓷和金属铌及不锈钢的扩散结合[J]. 材料科学与工艺,1998, 6(1):5—7.

[4] Kimura O, Kawashima T. Effect of interlayer thickness on residual thermal stresses in a ceramic-to-metal cylindrical joint[J]. Journal of the American Ceramic Society, 1993, 76(3): 757—759.

[5] Munz D, Sckuhr, Yang Y Y. Thermal stresses in ceramic-metal joints with an interlayer[J]. Journal of the America Ceramic Society, 1995, 78(2): 285—290.

[6] 汪建华,楼松年,戚新海,等. 陶瓷金属扩散焊接的残余应力及其缓和措施[J]. 硅酸盐学报,1995, 23(6): 606—609.

[7] 史耀武. 中国材料工程大典,第 3 卷[M]. 北京:化学工业出版社,2006.

[8] 贾成厂. 陶瓷基复合材料导论[M]. 北京:冶金工业出版社,2002.

作者简介:沈孝芹,女,1974 年出生,博士研究生,讲师。主要从事新材料及特种焊接技术的研究。发表论文 6 篇。

Email: 1921759594@163.com

ZHOU Xiaoling, SUN Jianchun (School of Materials Science & Engineering, Chongqing University, Chongqing 400030, China). p37—40

**Abstract**: Surface self-nanocrystallization (SSNC) by means of high energy shot peening (HESP) was applied to produce nanostructures on the ends of TA17 titanium alloy and 0Cr18Ni9Ti stainless steel bars, nanostructured surface layers were formed on the ends of samples. Making treated surfaces as interface, TA17 and 0Cr18Ni9Ti bars were bonded by impact pressure diffusion bonding (IPDB) on Gleeble—1500D tester. Joints were tested on tensile testing machine, the fractures and microstructures on the longitudinal section of joints were researched. Results shown that the maximum strength is about 384.0 MPa, brittle fracture is generated as the joints were tested, and the microhardness are varied with microstructures on the longitudinal section of joint.

**Key words**: surface self-nanocrystallization; titanium alloy; stainless steel; diffusion bonding; impact pressure

**Stress distribution in $Al_2O_3$-TiC/1Cr18Ni9Ti diffusion bonded joint** SHEN Xiaoqin[1,2], LI Yajiang[1], Puchkov U A[3], WANG Juan[1] and HUANG Wanqun[1] (1. Key Lab of Liquid Structure and Heredity of Materials, Ministry of Education, Shandong University, Jinan 250061, China; 2. School of Mechatronics, Shandong Jianzhu University, Jinan 250101, China; 3. Materials Science Department, Bauman Moscow State Technical University, Moscow 105005, Russia). p41—44

**Abstract**: The stress distribution of $Al_2O_3$-TiC/1Cr18Ni9Ti diffusion bonded joint was calculated using the finite element method and the effects of bonding temperature, pressure and interlayer on the stress distribution were studied. The results indicate that the axial stress and the shear stress both change greatly near the sample edge, which uniform near the center. The greatest shear stress occurs at the $Al_2O_3$-TiC/interlayer interface. The greatest axial tensile stress shifts from the ceramic side on the sample edge to the steel side near the edge and the value increases with the temperature decreasing. The axial compressive stress increases when the bonding temperature reduces. The increasement of the pressure can reduce the maximal axial tensile stress and improve the compressive stress. The change of the pressure has little effect on the shear stress. Both of the axial tensile stress and the shear stress decrease with Ti-Cu-Ti interlayer compared with Ti interlayer.

**Key words**: $Al_2O_3$-TiC; stainless steel; diffusion bonding; stress

**Numerical simulation of friction stir welding for aluminum alloy railway carriage manufacturing** ZHU Wenfeng[1], XU Chun[2] (1. School of Mechanical Engineering, Tongji University, Shanghai 200092, China; 2. Shanghai Institute of Technology, Department of Material, Shanghai 200235, China). p45—49

**Abstract**: High speed railway (HSR) uses aluminum hollow extrusions as new material and friction stir welding (FSW) is an innovative solid phase welding for such carriage manufacturing. Considering both the heat generation from tool shoulder friction and plastic deformation near the tool pin, a dual source finite element model of FSW is presented and a variety of weld joint designs are realized which satisfy the feature of FSW for the double skinned extrusion aluminum alloy structure. By ANSYS-APDL based re-exploitation, moving heat sources simulation is realized, and temperature field is obtained during the welding. The calculated results are in good agreement with experimental data, which indicate the model's feasibility and accuracy. It will benefit the digestion & assimilation of domestic-made level HSR vehicle manufacturing technology and provide reference for FSW process parameters optimization.

**Key words**: dual heat source; friction stir welding; aluminum alloy railway carriage; numerical simulation

**Granularity effect to E4303 electrodes' performance** GU Lingyan[1], XU Yuelan[1], ZHANG Xia[2], TANG Zhining[2] (1. Department of Materials Science and Engineering, Nanjing University of Science and Technology, Nanjing 210094, China; 2. Nanjing Lin Ken Equipment Limited Liability Company, Nanjing 210005, China). p50—52, 56

**Abstract**: Three different electrodes with different granularities medium carbon ferromanganese had been studied. The researches include welding technology performance of electrodes, the microstructure of deposited metal, chemical composition and impact toughness of deposited metal. The results showed that by adding nano medium carbon ferromanganese, the arc stability is better, the nano granule can increase nucleation core of crystal which play a role in grain refining, meanwhile the nano grain is burned badly, the deoxidation and desulfidation are weaken, impact toughness of deposited metal is reduced due to the overabundance oxide slag.

**Key words**: electrode; granularity; medium carbon ferromanganese

**Fatigue life prediction for flip chip soldered joints based on creep stain model** SHENG Zhong, XUE Songbai, ZHANG Liang, GAO Lili (Coolege of Materials Science and Technology, Nanjing University of Aeronautics and Astronautics, Nanjing 210016, China). p53—56

**Abstract**: Finite element method was used to simulate the inelastic stress in soldered joints of flip chip, and the results indicated that the maximums of equivalent creep strain and equivalent plastic strain in soldered joint both located at the upper surface of limbic chip. Processing the stress and strain of soldered joints with time, it was indicated that soldered joints had significantly relaxed the stress in the initial stage of circulation, with the accumulated trends of plastic strain and creep strain. With the hysteresis loop of stress-strain, cyclical variation of the loop was observed, and the curve became stable with the cyclic loading of heat. On account of the interaction between plastic strain and creep strain, the solomon model and shine and fox model were utilized to calculate fatigue life of the soldered joints. The simulated results were almost the same with the the practical life.

**Key words**: finite element method; plastic stain; creep stain; fatigue life

**Grain growth in heat affected zone of fine grained titanium alloy** WU Wei, GAO Hongming, CHENG Guangfu, WU Lin (State Key Laboratory of Advanced Welding Production Technology, Harbin Institute of Technology, Harbin 150001, China). p57—60, 64

**Abstract**: Grain growth in coarse grained region of fine grained titanium alloy welded joint was studied, and influences of